Proceedings of the ASME 2021
48th Annual Review of Progress in
Quantitative Nondestructive Evaluation
QNDE2021
July 28-30, 2021, Virtual, Online

QNDE2021-74931

RESEARCH ON KEY TECHNOLOGIES OF PRECISE MEASUREMENT OF GEOGRAPHIC COORDINATES OF SUBSEA PIPELINES

Li Jian[1], Wang Jialin[1], Zhao Jianyuan[2], Li Mingze[1], Huang Xinjing[1]*

[1]State Key Laboratory of Precision Measuring Technology and Instruments, Tianjin University, Tianjin 300072, China
[2]AECC AERO Engine Control System Institute, Wuxi 214063, China
*: Corresponding author, huangxinjing@tju.edu.cn (Huang Xinjing)

ABSTRACT

With the continuous increase of offshore oil and gas exploitation activities, the number of subsea pipelines is becoming larger and larger, which leads to frequent occurrence of subsea pipeline accidents. Long-term safe operation of subsea pipelines can be ensured by regular defect detection. The premise of locating and disposing defects is to accurately measure the geographic coordinates of subsea pipelines. Our research group has put forward a kind of pipeline spherical internal detector (SD), which has the advantages of convenient implementation, low risk to jam. For the SD, this paper has carried out research on the key technology of precise measurement of subsea pipelines' geographic coordinates using the internal magnetic fields. The main work is as follows:

(1) Magnetic tensor invariant calibration method for magnetometer array has been studied and L-M algorithm is taken to solve the parameters, which is efficient and accurate. Field calibration experiment has proved this method is effective and has good robustness.

(2) A new method of measuring pipeline's pitch angle is proposed. Under the experimental condition of using AC servo motor to drive the sensor instead of the SD to rotate, the pitch angle measurement error is less than 0.2°.

(3) Magnetic anomaly of spiral weld and buckling pipeline are used as new mark points to calibrate the geographic coordinates of subsea pipelines. Experimental results show that the newly designed SD can successfully identify spiral welds and buckling pipeline.

Keywords: Subsea pipeline, Geographic coordinates, Magnetic sensor calibration, Pitch angle, Spherical inner detector

1. INTRODUCTION

In recent years, the focus of global offshore oil and gas exploration and development is gradually moved to deep-water areas [1]. Pipeline transportation is mostly used to transport offshore oil and gas to onshore oil depots. However, the subsea pipeline is not completely safe. In case of leakage, due to the complexity of the seabed environment, pipeline leakage cannot be found at the first time, oil and gas will spread very fast in the marine environment, which may lead to ecological disasters. Therefore, timely and regular inspections of subsea pipelines are required, which needs to geographic coordinates measurement of the pipeline. This can timely grasp the deformation and drift, quickly locate and repair the fault, effectively reduce the risk of scratch and collision in offshore operation, and provide more timely safety warning.

At present, there are two main methods of subsea pipeline geographic coordinate measurement: external detection method and internal detection method. The external detection method employs ROV and AUV to accurately locate obvious external defects of subsea pipelines and determine their position through the navigation system. However, due to deployment difficulty, high cost and long detection cycle of the external detection method, people focus on the internal detection method and successfully develop the PIG which can run inside the pipeline. Due to the shielding effect of seawater and pipeline, GPS and AGMs cannot be used by PIG for positioning calibration. Moreover, the PIG has a risk of blockage because of its large volume and weight. In recent years, our research group has proposed a positioning method using the spherical internal detector (SD) [2]-[7]. This location method is convergent, and its accuracy is independent of mileage. Because the outer diameter of the SD is much smaller than the inner diameter of the pipeline, it has good trafficability. Moreover, the SD has the advantages of

low power consumption, low cost, high resolution and quasi real-time measurement.

The method of using the SD to measure the geographic coordinates of subsea pipelines is based on coordinate inversion using the acceleration and the magnetic field data recorded by the SD in the pipeline [2]. The direction of the pipeline can be determined by the horizontal angle and pitch angle in the world coordinate system based on the magnetic shielding model of the ferromagnetic steel pipeline. After the pipeline direction is obtained from the two angles and combined with the mileage obtained from the acceleration data, the geographic coordinates of the pipeline can be calculated. As the internal magnetic field should be measured very precisely in order to accurately calculate the pipeline direction, the magnetometer array needs to be calibrated. In addition, it is necessary to detect some mark points on the pipelines to correct the mileage error of the SD. It is also beneficial to accurate pipeline geographic coordinates measurement if the pipeline pitch angle can be independently measured.

2. IMPROVEMENT SCHEME

In order to improve subsea pipeline's geographic coordinate measurement using the SD, this paper makes a targeted research, as shown in Figure 1. It mainly includes the following three points:

(1) Improve the accuracy of magnetic field measurement inside the pipeline. The positioning model used in this paper is the magnetic shielding model. At present, the magnetometers used for measurement have not been calibrated, which will lead to the measurement error of the pipeline orientation. Therefore, the calibration algorithm of the magnetometer is studied to improve the measurement accuracy of the internal magnetic field of the subsea pipeline.

(2) Improve the measurement accuracy of pipeline's pitch angle. A new measurement method of pipeline's pitch angle based on AC magnetic proximity switch is proposed to improve the accuracy of measurement.

(3) Improve the mileage measurement accuracy of the SD. A new SD is designed to identify spiral weld and pipeline buckling as position marking point.

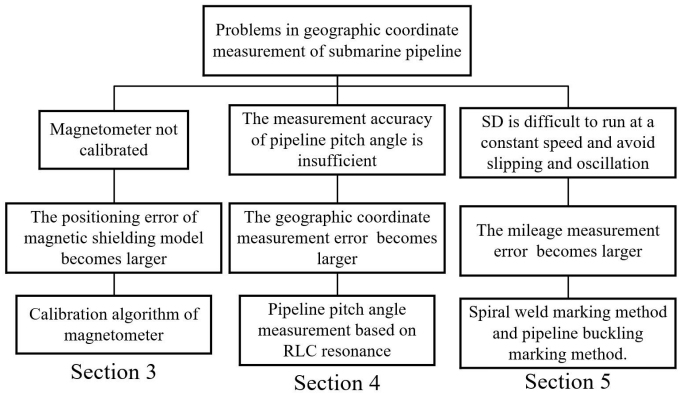

FIGURE 1: RESEARCH CONTENTS OF EACH SECTION

3. CALIBRATION ALGORITHM OF MAGNETOMETER

Measurement of subsea pipeline geographic coordinates uses magnetic shielding model to identify the trend of subsea pipeline. This requires that the magnetic field inside the pipeline measured by the spherical internal detector is accurate enough. The installation error and triaxial angle deviation of the magnetometer sensor need to be calibrated. Therefore, the calibration algorithm of the magnetometer is studied and verified to calibrate the comprehensive error of the magnetometer.

3.1 Principle of calibration algorithm

3.1.1 Magnetic gradient tensor invariant

The calibration principle in this paper is based on the magnetic gradient tensor variable. The magnetic gradient tensor is the derivative of the components *Bx*, *By*, *Bz* of the space magnetic field vector *B* in the *x*, *y*, *z* directions, as shown in formula (1).

$$G = \begin{bmatrix} \partial/\partial x \\ \partial/\partial y \\ \partial/\partial z \end{bmatrix} [B_x \quad B_y \quad B_z] = \begin{bmatrix} B_{xx} & B_{xy} & B_{xz} \\ B_{yx} & B_{yy} & B_{yz} \\ B_{zx} & B_{zy} & B_{zz} \end{bmatrix} \tag{1}$$

If the background magnetic field can ensure short-term stability, it can be regarded as a passive quasi-static magnetic field with curl and divergence of 0 [8], which is formula (2).

$$\begin{aligned} \nabla \times B &= 0 \\ \nabla \bullet B &= \frac{\partial B_x}{\partial x} + \frac{\partial B_y}{\partial y} + \frac{\partial B_z}{\partial z} = 0 \end{aligned} \tag{2}$$

Therefore, only five components of the magnetic gradient tensor are independent of each other. *G* can be expressed as formula (3).

$$G = \begin{bmatrix} B_{xx} & B_{xy} & B_{xz} \\ B_{xy} & B_{yy} & B_{yz} \\ B_{xz} & B_{yz} & -B_{xx} - B_{yy} \end{bmatrix} \tag{3}$$

Magnetic gradient tensor invariants are constants that do not follow the coordinate system after the magnetic gradient tensor components are rotated [9]-[11], including norm, determinant and sum of squares. The norm C_T selected in this paper is expressed as formula (4).

$$\begin{aligned} C_T &= \sqrt{\sum_{i,j=x,y,z} B_{ij}^2} = \sqrt{-2I_1} \\ I_1 &= B_{xx}B_{yy} + B_{yy}B_{zz} + B_{zz}B_{xx} - B_{xy}^2 - B_{yz}^2 - B_{zx}^2 \end{aligned} \tag{4}$$

3.1.2 Error model of magnetic gradient field

The relationship between the magnetic field values measured by the three-axis vector magnetic sensor and the true values is shown in the formula (5) [11]:

$$B_m = M_s M_f M_o (B_t + h) + b \tag{5}$$

Wherein B_m is the measured value; B_t is the true value; M_f is the scale error; M_o is a tri-axis non-orthogonal error; M_s and h are errors of soft and hard iron; b is the bias error.

For the cross-type magnetometer array, the magnetic vector gradient after calibration is shown as formula (6).

$$\partial B_x = \frac{(B_{t1} - R B_{t3})}{d} \approx \frac{\left(B_{m1} - R\left(M_s M_f M_o (B_{m3} + h) + b\right)\right)}{d} = \frac{(B_{m1} - T_{13} B_{m3} - E_{13})}{d} \tag{6}$$

Wherein, ∂B_x is the gradient of the x component of the magnetic vector B, and R is the mismatch error.

Combining the formulas (4), the function of parameter I_1 in the magnetic gradient tensor variable C_T used for calibration is obtained as formula (7).

$$I_1 = f\left(B_{xx}, B_{yx}, B_{zx}, B_{xy}, B_{yy}, B_{zy}\right) = f(T_{13}^{3\times3}, E_{13}^{3\times1}, T_{24}^{3\times3}, E_{24}^{3\times1}) \tag{7}$$

The basic idea of calibration is that no matter how the magnetic array rotates around its center, the C_T remains the same, then I_1 remains unchanged. When the calibration is actually performed, the I_1 calculated from N sets of sample points collected during the rotation process is minimized to solve the parameters, that is expressed as formula (8).

$$min \sum_{i=1}^{N} |f_i(T_{13}^{3\times3}, E_{13}^{3\times1}, T_{24}^{3\times3}, E_{24}^{3\times1}) - c|^2 \tag{8}$$

This is a nonlinear optimization problem with 25 unknown parameters, where c is a constant.

3.2 Experiment of magnetic gradient tensor invariant calibration

The magnetic field characteristics measured by each sensor in the magnetic array are similar. The data is calibrated, and the parameter solution algorithm uses L-M algorithm.

The change of C_T value before and after calibration and F value of objective function during L-M algorithm iteration are shown in Figure 2, and the statistical characteristics of C_T value before and after calibration are shown in Table 1.

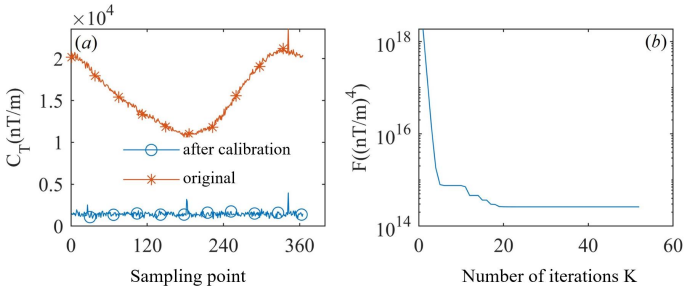

FIGURE 2: CALIBRATION RESULTS: (a) Comparison of C_T value before and after calibration (b) Change of F value of objective function with iteration times

TABLE 1: STATISTICAL COMPARISON OF C_T VALUE BEFORE AND AFTER CALIBRATION

C_T value	Before calibration	After calibration	after/before
average (nT/m)	15769	1433	0.091
RMS (nT/m)	3472	279	0.081

Background magnetic fields range from complex to uniform, and the fluctuations of C_T values after calibration at any location are reduced by 10-23 times than before, which shows that the magnetic gradient tensor invariant calibration method is feasible and has good robustness. L-M algorithm also has good robustness in solving the calibration parameters of magnetic gradient tensor invariants. It is an efficient algorithm. In the experiment, the maximum number of iterations is no more than 63, and the average number of iterations is 52.

4. MEASUREMENT OF PIPELINE'S PITCH ANGLE

4.1 Principle of pipeline's pitch angle measurement

The subsea pipeline will pitch with the fluctuation of the seabed. Therefore, the pitch angle needs to be measured as accurately as possible to correctly measure the geographic coordinates of the subsea pipeline. This paper presents a new method for pipeline's pitch angle measurement based on AC magnetic proximity switch formed by the SD and RLC resonant coils.

The principle of pipeline's pitch angle detection is based on RLC series resonance amplification and eddy current effect. The measurement method is shown in Figure 3. The SD carries RLC resonance detection coils and a triaxial accelerometer chip. The sensitive axis direction of the accelerometer is located at the connecting line between the coil center and the SD center to obtain the direction of gravity acceleration g.

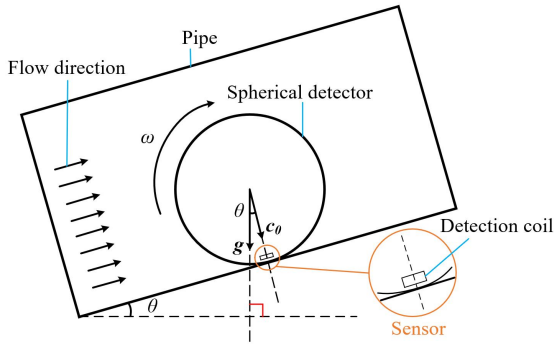

FIGURE 3: PRINCIPLE OF PIPELINE'S PITCH ANGLE MEASUREMENT

When the coil is closest to the inner wall of the pipe, the connecting line between the coil center and the SD center is just perpendicular to the inner wall of the pipe. At this moment, the

coil output voltage is the minimum value c_0. Therefore, the pipeline's pitch angle θ can be expressed as formula (9).

$$\theta = \pm cos^{-1}(c_o/g) \tag{9}$$

According to this method, the pitch angle of the pipeline is calculated by the phase difference between the extreme values of the coil output and the accelerometer signal.

4.2 Experiment of pipeline's pitch angle measurement

The experiment of pipeline's pitch angle measurement under laboratory conditions is carried out as shown in Figure 4, and the results are shown in Figure 5. In the experiment, an AC servo motor was used to drive the sensor instead of the SD to rotate.

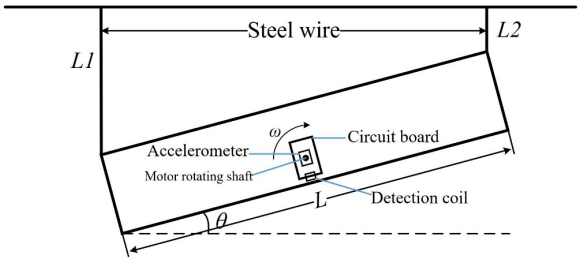

FIGURE 4: EXPERIMENT OF PIPELINE'S PITCH ANGLE MEASUREMENT

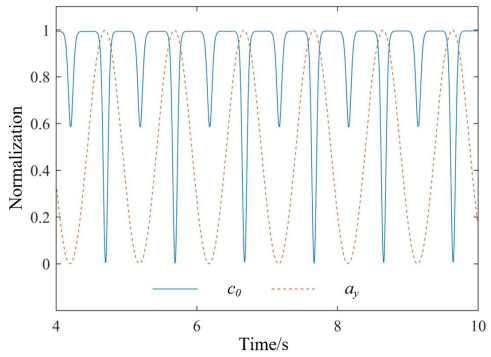

FIGURE 5: EXPERIMENTAL RESULTS OF PIPELINE'S PITCH ANGLE MEASUREMENT

Since the sensor will approach the inner wall of the pipe twice during one rotation, there are two extreme values in the coil output signal: the first approach to the inner wall at the bottom of the pipe corresponds to the smaller of the two extreme values, and the second approach to the inner wall at the top corresponds to the larger one.

Processing the data, includes removing gross error, signal filtering and normalization, then detecting the extreme point, calculating the phase difference between the extreme point of acceleration and coil signal, and finally calculating the pipeline's pitch angle. As shown in Table 2, the measurement error of pipeline's pitch angle is within 0.2°, so the designed pitch angle measurement sensor has high accuracy.

TABLE 2: EXPERIMENTAL MEASUREMENT RESULTS

L1/(mm)	L2/(mm)	L/(mm)	Actual/(°)	measured/(°)	error/(°)
132	127	600	0.478	0.622	0.144
111	149	600	-3.631	-3.816	-0.185
106	155	600	-4.684	-4.792	-0.108
90	168	600	-7.470	-7.513	-0.043
55	209	600	-14.872	-14.943	-0.071
44	224	600	-17.458	-17.228	0.230
9.4	277	600	-26.487	-26.551	-0.064
74	401	600	-33.025	-32.978	0.047
63	430	600	-37.710	-37.702	0.008
43	468	600	-45.100	-45.114	-0.014

5. IMPROVEMENT OF MILEAGE MEASUREMENT ACCURACY

5.1 Principle of improving mileage measurement accuracy

Using the SD to accurately obtain the geographic coordinates of subsea pipeline needs to accurately measure the mileage. The previous calculation method of mileage is shown in the formula (10).

$$\begin{aligned} v(t) &= \omega(t) r_b = \pi D_b f(t) \\ s(t) &= \int_0^t \pi D_b f(t) dt \end{aligned} \tag{10}$$

Where r_b and D_b are the radius and diameter of the SD respectively, and f is the rolling frequency of the SD in the pipe.

The premise of the above mileage calculation method is that the SD rotates at a uniform speed and there is no slip and spherical oscillation, which is difficult to realize in reality. Based on the above problems, two new methods to correct mileage error through the marking points of the pipeline itself are proposed: spiral weld marking method and buckling pipeline marking method.

The spiral weld marking method is used to mark mileage error with equal spacing of spiral pipe welds. The distance of the SD fixed axis rolling for one circle is its circumference, which corresponds to one cycle of acceleration signal. The acceleration signal can be used to calculate the mileage - time curve of the SD. Since the time of magnetometer and accelerometer are aligned, the axial position of spiral weld can be determined by comparing mileage - time curve and magnetic characteristic - time curve.

The buckling pipeline marking method is applicable to all kinds of ferromagnetic pipelines. It compares the known geographic coordinates of the buckling of pipeline with the measured one to correct the mileage error.

The premise of these two calibration methods is that the SD can identify the pipeline marking points and record the location of them. Therefore, the next section will describe in detail how to identify spiral welds and buckling pipeline marking points with the SD.

5.2 Experiments of Magnetic Anomaly Detection

5.2.1 Spiral weld detection

The experiment of using the SD to locate the spiral weld position is shown in Figure 6. The SD rolls forward in the pipe to measure the magnetic field inside the pipe. By rotating the spiral pipe around the axis, different spiral weld positions can be obtained. Four rotation tests were performed.

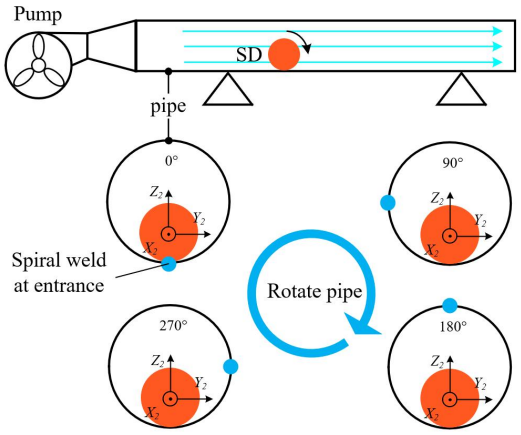

FIGURE 6: EXPERIMENT OF LOCATING SPIRAL WELD

Because the magnetic component B_y is collinear with the rolling axis of the SD, the fluctuation is small, which can well indicate the distribution of lateral magnetic field inside the pipeline. B_y contains a very obvious concave magnetic feature, which corresponds to the spiral weld. Cubic processing of B_y can suppress the interference signal and enhance that of weld signal.

The results of the internal magnetic component B_y of the spiral pipe at different rotation angles are shown in Figure 7. It can be found that the lateral magnetic field B_y has a depression feature at the spiral weld, which is more obvious after cubic enhancement. Therefore, this method can effectively identify spiral welds.

The dual channel design can not only determine the rotation direction of spiral pipe, but also eliminate the influence of interference peak and improve the recognition rate of spiral weld.

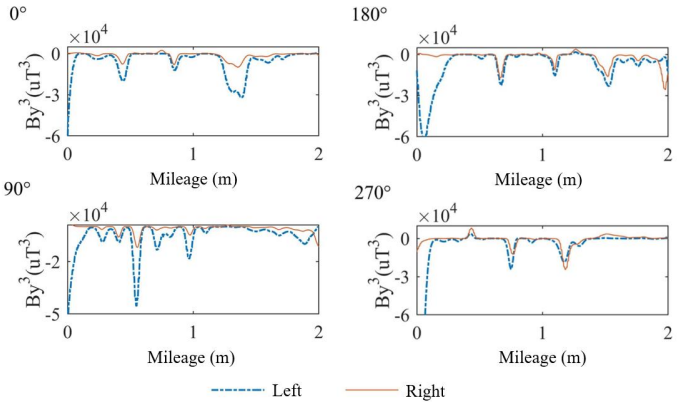

FIGURE 7: MEASUREMENT RESULTS OF INTERNAL LATERAL MAGNETIC FIELD OF SPIRAL PIPE AT DIFFERENT ANGLES

5.2.2 Pipeline buckling identification

The magnetic fields in the buckling pipe with different directions are measured. The experimental process is shown in Figure 8. Two kinds of buckling pipes were tested in the experiment, and the internal magnetic field of the straight pipe was used as the contrast. The pipeline parameters are shown in Table 3 and the measurement results are shown in Figure 9.

For the large buckling pipe 1#, the internal magnetic field of the pipe without demagnetization usually has a strong original magnetic field, which will mask or reduce the characteristic signal of the buckling, so demagnetization is carried out.

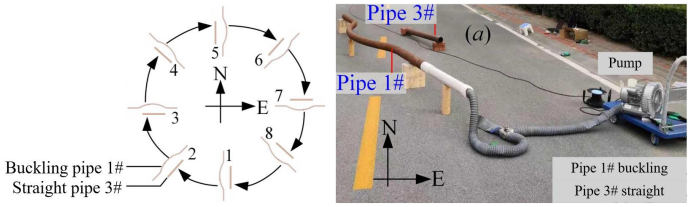

FIGURE 8: EXPERIMENT OF PIPELINE BUCKLING IDENTIFICATION

TABLE 3: PIPELINE PARAMETERS

Pipe	Type	L/m	Φ/mm	T/mm	$\overline{\theta}/^\circ$	$\theta_m/^\circ$
1#	Buckling	5	114	5	18.43	60
2#	Buckling	2	80	4	17.74	45
3#	Straight	2	114	5	--	--

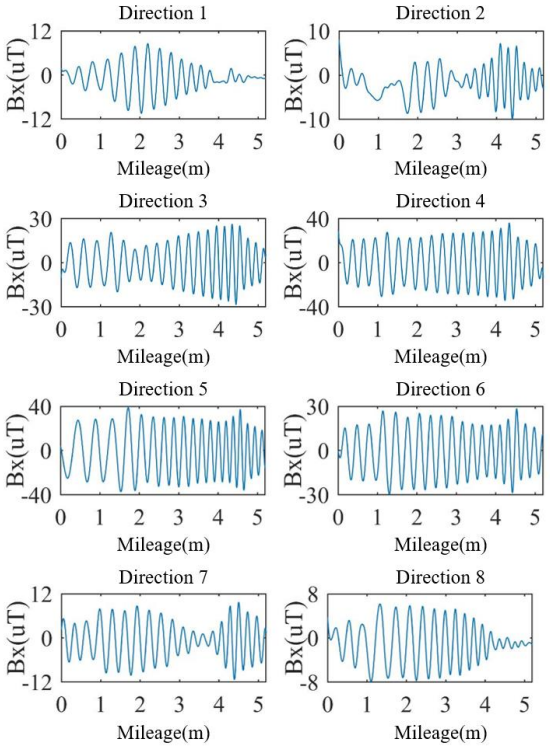

FIGURE 9: MAGNETIC FIELDS INSIDE BUCKLING PIPE 1# IN DIFFERENT DIRECTIONS AFTER DEMAGNETIZATION

Through comparison, it can be seen that unlike the relatively uniform internal magnetic field of a straight pipe, for most directions, there will be one or two characteristic peaks in the internal magnetic fields of the buckling pipe. Although these characteristic peaks have different shapes, they can be clearly distinguished from the magnetic fields in the straight pipe, which can clearly indicate the existence of buckling. Therefore, it is feasible to identify buckling pipeline by the SD.

6. CONCLUSION

(1) It is feasible to apply the magnetic gradient tensor invariant calibration algorithm to calibrate the magnetometer array, and the fluctuation degree of CT value after calibration is greatly reduced.

(2) The new method for measuring pipeline's pitch angle is feasible. In this method, the RLC series resonant circuit is used to increase the measurement sensitivity, detect the time when the coil points to the pipe wall, and calculate the pitch angle combined with the output of the accelerometer.

(3) This paper has also demonstrated a method to correct mileage error by using spiral weld and buckling pipeline as marking points, and successfully identifies them.

ACKNOWLEDGEMENTS

This work is supported by National Natural Science Foundation of China (Nos. 62073233, 61773283, 61973227).

REFERENCES

[1] Niu A, Bi Z, Zhang G. Development and Application of Pipeline Steel and Steel Pipe for Offshore Pipeline in China. Welded Pipe and Tube, 2019, 42(6): 1-6.

[2] Huang X. Research on Geographic Coordinate Measurement of Subsea Pipelines. Dissertation of Tianjin University. Tianjin, China. 2016.

[3] Huang X., Chen S., Guo S. et al. A 3D Localization Approach for Subsea Pipelines Using a Spherical Detector. IEEE Sensors Journal, 2017, 17(6): 1828-1836.

[4] Huang X., Chen G., Zhang Y. et al. Inversion of magnetic fields inside pipelines: modeling, validations, and applications. Structural Health Monitoring, 2018, 17(1): 80-90.

[5] Zhang Y., Xue Y., Huang X. et al. Characterizations of magnetic field distributions inside buckling pipelines. Applied Computational Electromagnetics Society Journal, 2018, 33(12): 1475-1482.

[6] Zhang Y., Xue Y., Huang X. et al. Pipeline inclination measurements based on a spherical detector with magnetic proximity switches. IEEE Access, 2018, 6: 39936-39943.

[7] Guo L., Zeng Z., Huang X. et al. Vibration Detection of Spanning Subsea Pipelines by Using a Spherical Detector. IEEE Access, 2019, 7: 7001-7010.

[8] Leslie K E., Foss C., Hillan D., et al. A Downhole Magnetic Tensor Gradiometer for Developing Robust Magnetisation Models from Magnetic Anomalies. Iron Ore 2015: 1-11.

[9] Mu Y., Wang C, Zhang X. et al. A Novel Calibration Method for Magnetometer Array in Nonuniform Background Field. IEEE Transactions on Instrumentation and Measurement, 2019, 68(10): 3677-3685.

[10] Sui Y., He W., Xia Z. et al. Error Analysis and Correction of a Downhole Rotating Magnetic Full-Tensor Gradiometer. IEEE Access, 2020, 8: 127-139.

[11] Wang X., Liu Y., Ouyang J. et al. Calibration method for mismatch error of a magnetometer array based on two excitation coils and the particle swarm optimization algorithm. Measurement Science and Technology, 2020, 31(11).